Microwave Absorption of Single-Walled Carbon Nanotubes/Soluble Cross-Linked Polyurethane Composites

Zunfeng Liu,[†] Gang Bai,[†] Yi Huang,[†] Feifei Li,[‡] Yanfeng Ma,[†] Tianying Guo,[†] Xiaobo He,[§] Xiao Lin,[§] Hongjun Gao,[§] and Yongsheng Chen*,[†]

Key Laboratory of Functional Polymer Materials and Center for Nanoscale Science and Technology, Institute of Polymer Chemistry, The College of Chemistry, Nankai University, The College of Physics, Nankai University, Tianjin 300071, China, and The Institute of Physics, Chinese Academy of Sciences, eijing 100080, China

Received: April 24, 2007; In Final Form: June 29, 2007

Processable composites of single-walled carbon nanotubes (SWNTs) with soluble cross-linked polyurethane (SCPU) were prepared at various loadings of SWNTs (0−25 wt %), and they exhibited strong microwave absorption in the microwave range of 2−18 GHz. For example, 5 wt % loading SWNTs/SCPU composite has a strong absorbing peak at 8.8 GHz and achieves a maximum absorbing value of 22 dB. The absorbing peak position moves to lower frequencies with increasing SWNT loading. Theoretical simulation for the microwave absorption using the transmission line theory agrees well with the experimental results. The microwave absorption of these composites can be mainly attributed to the dielectric loss rather than magnetic loss.

1. Introduction

Microwave-absorbing materials are currently in high demand for many expanded electromagnetic interference (EMI) shielding and radar cross section (RCS) reduction applications with both commercial and defense purposes. Consumer electronics, computers, wireless LAN devices, wireless antenna systems, and cellular phone systems are just a few device applications that require these materials. Generally, magnetic or metal particles are used for the microwave absorption materials. However, high specific gravity and difficult formulation have limited their practical applications. Thus, there remains a need for an efficient microwave-absorbing material that is relatively lightweight, structurally sound and flexible, and efficient in absorption in a wide band range. The nanostructured materials have attraction for microwave radiation absorbing and shielding materials in the high-frequency range due to their many unique chemical and physical properties.[1−4] Particularly, the unique structure and many excellent properties of carbon nanotubes (CNTs), including single-walled and multiwalled carbon nanotubes (SWNTs and MWNTs) have prompted intensive studies for many potential engineering,[5−10] including EMI shielding, applications.[11−17] Recent studies have demonstrated that MWNTs show strong microwave absorption with a matrix of polyethylene terephthalate (PET)[13] and poly(ureaurethane) (PU),[18] and multilayered radar-absorbing structures of MWNT-filled composites have been designed for the X-band range (8.2−12.4 GHz).[19] The electrical properties of small diameter SWNTs are distinctly different from their larger diameter MWNT counterparts due to their smaller diameters and larger aspect ratios. Thus, per unit wt % added to the polymer matrix, the nature of the EM-absorbing properties of MWNT− and SWNT−polymer composites is expected to be altogether different. We were therefore motivated to study the EM-absorbing properties and applications for SWNT composite materials and found that these composites showed strong microwave-absorbing properties and could be used as radar-absorbing materials in a wide frequency range.

Polymeric materials have been largely used as a matrix for EMI studies partially because of their easy fabrication into various shapes.[20−24] Polyurethanes (PUs), with possessing advantages such as excellent mechanical properties, good biocompatibility, design flexibility, light weight, and low cost, have a wide range of applications such as coatings, adhesives, sealants, and composites. For example, utilizing the unique electric and heat properties of PU and MWNTs, Koerner et al. recently prepared a remotely actuated stress-recovery material with over 50% recovery stress.[25]

In our previous studies,[11,26] we have found that SWNTs/epoxy composites show excellent EMI shielding effectiveness and could be used as an effective lightweight EMI shielding material for uses such as mobile phone systems that operate near ∼1 GHz. Here, we report the first results of microwave absorption studies of the SWNTs−polymer composites using a soluble cross-linked polyurethane (SCPU)[27] as the matrix. The reason we chose SCPU is to have both better processing and mechanical properties for the potential future commercial applications. The new soluble SCPU, made by a mainly intramolecular cross-linking step, could be easily processed using a solution or hot-pressing process.[27]

2. Experimental Section

2.1. Materials. SWNTs were prepared in our laboratory with a modified arcing method at large scale using Ni/Y as catalyst.[28] *N*,*N*-Dimethylformamide (DMF) was dried under molecular sieves (4A) and distilled under reduced pressure. Hydroxy-terminated polybutadine (HTPB) (hydroxyl number, 0.767 mmol/g; M_n, 2600) was used as purchased (Zibo Qilong Chem Co, China). All other materials were used as purchased.

* To whom correspondence should be addressed. Tel.: +86 (22) 2350-0693. Fax: +86 (22) 2349-9992. E-mail: yschen99@nankai.edu.cn.
[†] College of Chemistry, Nankai University.
[‡] College of Physics, Nankai University.
[§] Chinese Academy of Sciences.

10.1021/jp0731396 CCC: $37.00
Published on Web 08/29/2007

2.2. Preparation of SWNTs/SCPU Composites. Cross-linked PUs have better mechanical properties and are in high demand for many applications, but conventional cross-linked PUs are insoluble and hard to process. In view of recent progress making soluble SCPU, a new soluble SCPU with a diol soft segment was synthesized similarly using a literature method[27] for our SWNT composites. The SWNTs/SCPU composite with 5 wt % SWNTs was fabricated as follows. To a dried round-bottom flask with melted diphenylmethane diisocyanate (MDI) (12.76 g, 0.051 mmol) was added dropwise HTPB (66.4 g, 0.026 mmol) with stirring at 60 °C, and the mixture was stirred further for 1 h at 60 °C. A volume of 30 mL of DMF was then added to dilute the rather sticky mixture to generate a diluted homogeneous solution, and 1.606 g (0.018 mmol) of 1,4-butadiol (BD) was added dropwise with stirring. The mixture was stirred at 60 °C for 1 h, and then the temperature was kept at 80 °C for 2 h. During this 3 h period, 300−500 mL DMF/toluene (vol ratio: 1/4) mixed solvent was added gradually to reduce the viscosity of the mixture. In order to complete the cross-linking reaction, the temperature was raised to 90 °C and kept for 2 h. Then the dispersed suspension with 4.25 g SWNTs in DMF/toluene (1/4, 100 mL) was added gradually into above SCPU DMF/toluene solution with stirring to yield a homogeneous composite solution/suspension and then poured into a container with size of 180 mm × 180 mm × 150 mm. After almost all solvent was evaporated at 90 °C, the film was vacuum-dried at 120 °C for 24 h and then pealed off. A hot pressure process at 170 ×bcC and 15 MPa using the same mold of 180 mm × 180 mm × 2 mm was then applied to get a smooth flat sheet for the following measurements. SWNTs/SCPU composites with other loading from 0.01% to 25% were fabricated in the similar process. The molar ratio of HTPB/MDI/BD was 1/2/0.7 for all composites. A control sample was also made in the same way without SWNTs for comparison.

2.3. Instruments and Measurements. The scanning electron microscopy (SEM) images were obtained using a Hitachi S-3500N scanning electron microscope. The dc electrical conductivity of the SWNTs/epoxy composites was determined using the standard four-point contact method on rectangular sample slabs in order to eliminate contact-resistance effects. Data were collected with a Keithley SCS 4200. The relative complex permittivity $\epsilon = \epsilon' - j\epsilon''$ and relative complex permeability $\mu = \mu' - j\mu''$ were determined using the *T*/*R* coaxial line method in the range of 2−18 GHz with an O-ring shaped sample (i.d. = 3 mm and o.d. = 7 mm, thickness = 2 mm) using an HP8722ES vector network analyzer. The microwave-absorbing characteristics were evaluated by measuring the reflection loss using an HP8757E scalar quantity network analyzer in the 2−18 GHz band range, and the sample sheets (180 mm × 180 mm × 2 mm) were mounted onto an aluminum substrate. All the measurements were performed at room temperature.

3. Results and Discussion

3.1. Conductivity of SWNTs/SCPU Composites. Figure 1 shows the dc conductivity (σ) of SWNTs/SCPU composites as a function of SWNTs mass fraction (p) in a logarithmic scale. It can be seen that the conductivity displays a dramatic increase below 5 wt %, indicating the formation of a percolating network. The inset in Figure 1 shows that the electrical conductivity obeys the power law:[29]

$$\sigma \propto (\nu - \nu_c)^{\beta} \qquad (1)$$

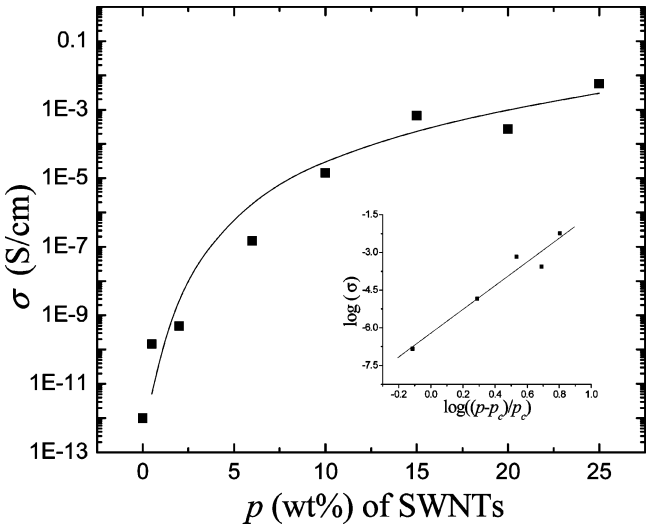

Figure 1. log dc conductivity (σ) vs mass fraction (p) of SWNTs/SCPU composites measured at room temperature. Inset: log−log plot of σ vs $((p - p_c)/p_c)$ for the same composites. The straight line in the inset is a least-squares fit to the data around the percolation point using eq 1, returning the best-fit values of $p_c = 3.4\%$ and $\beta = 4.7$.

where σ is the conductivity, ν is the volume fraction, ν_c is the percolation threshold, and β is the critical exponent. Since the densities of the polymer and the SWNTs are very similar, we assume that the mass fraction p and the volume fraction ν of the SWNTs are almost the same. As shown in the inset in Figure 1 for the $\log(\sigma)$ versus $\log((p - p_c)/p_c)$ plot, the conductivity of SWNTs/SCPU composite agrees very well with the percolation behavior predicted by eq 1. Although computer models of conductivity percolation give a critical exponent value of 1.5 for a rigid rod network,[30] various values from 1.3 to 5.3 have been reported for different CNT−polymer composites.[11,14,31] In our case, the straight line in the Figure 1 with percolation threshold $p_c = 3.4\%$ and critical exponent $\beta = 4.7$ gives an excellent fit to the data around the percolation threshold with a correlation factor of 0.97.

A percolation threshold of 3.4% is rather low compared with that of the three-dimensional (3D) percolation system composites (16%).[26] This can be attributed to the large aspect ratio of one-dimensional SWNTs compared to spheres (3D). However, such a percolation threshold of 3.4% is relatively higher compared with some CNT-related work[31,32] and much higher than that in our recent work[11] with epoxy as matrix (the p_c is 0.06%). From the SEM pictures in Figure 2 it can also be confirmed that the SWNTs were inhomogenously dispersed in SCPU matrix, in which SWNTs still aggregated to form large bundles. But it should also be pointed that both theory[29,30,33] and experimental[34] results for the percolation threshold (p_c) are in a wide range, depending on the filler's aspect ratio, processing methods, matrix and etc. The percolation value of 3.4% in our case is reasonable if our experimental details in the sample preparation process are considered: a viscous polymer solution where SWNTs were added and a slow drying process due to the high boiling point solvent DMF.

3.2. Microwave Absorption Properties of the SWNTs/SCPU Composites. The radar-absorbing ability for the composite was evaluated by measuring the reflection loss on an HP8757E scalar quantity network analyzer. During the measurement the sample sheet with a size of 180 mm × 180 mm × 2 mm was put on an aluminum substrate having the same dimension as the sample. A schematic representation of the measurement of wave-absorbing ability is shown in Figure 3.

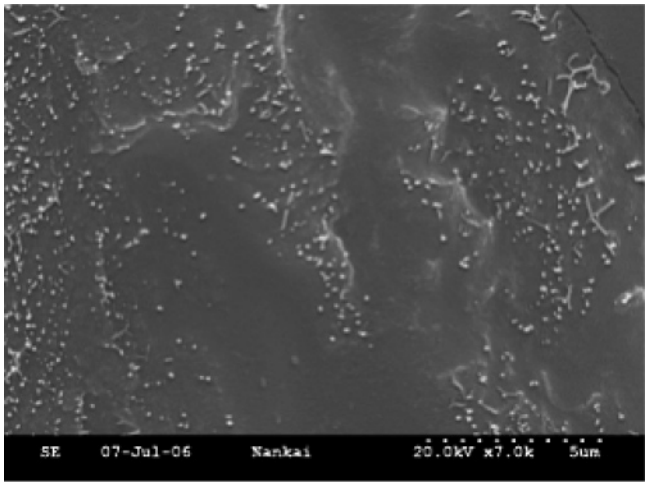

Figure 2. Typical SEM image of the SWNTs/SCPU composite with 20 wt % loading.

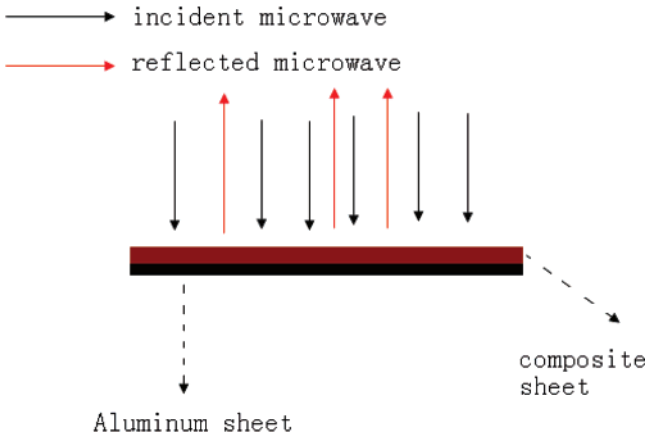

Figure 3. Schematic representation for the mechanism of the measurement of microwave absorption ability. Black arrows represent the incident microwave; the red arrows represent the reflected microwave. By measuring the intensity of the reflected microwave, we can evaluate the wave-absorbing ability of the composite. A weak reflected signal indicates a good wave-absorbing ability.

The composite sheet is placed on an aluminum substrate. The incident microwave is divided into two parts in our experiment: the reflected microwave and the absorbed one. If P_{in} is the incident power density at a measuring point before absorption, and P_R is the reflected power density at the same measuring point, P_A is the absorbed power by the composite, we can get

$$P_{in} = P_R + P_A \quad (2)$$

$$R = 10 \log P_R/P_{in} \quad (3)$$

$$A = 10 \log P_A/P_{in} \quad (4)$$

where R and A are the reflection loss and the absorption loss in decibels (dB), respectively. Here the microwave-absorbing efficiency can be evaluated from R. The larger the absolute value of R is, the stronger the wave-absorbing ability will be.

Figure 4 shows the experimental results of the reflection loss versus frequency for SWNTs/SCPU composites with the increase of SWNTs loading from 1 to 25 wt % in the range of 2−18 GHz. The composite film with a loading of 1 wt % shows weak wave-absorbing ability, and the absorption peak increases to 13.3 dB at the loading of 2 wt % and then reaches the

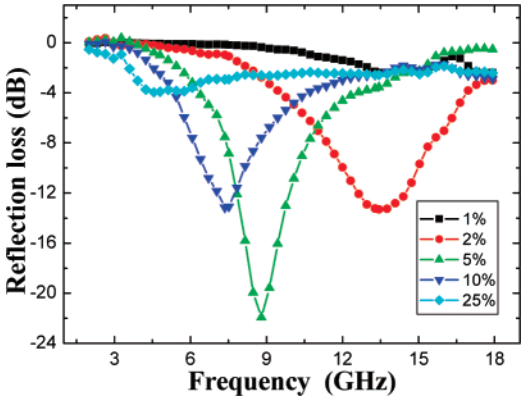

Figure 4. Reflection loss of SWNTs/SCPU composites of different loadings vs frequency.

maximum value of 21.9 dB at the loading of 5 wt %. But with further increasing SWNT loading, the wave-absorbing ability decreases. We argue that further increase of SWNT loading (after 5 wt %) could cause more reflection due to the shorter distance of resonance multipoles with more SWNTs loaded.[13] Also, it is clearly seen that the peak position moves to lower frequencies with increasing SWNT concentrations. For example, the strong absorption ranges (>10 dB, e.g., over 90% microwave absorption) are 6.4−8.2, 7.5−10.1, and 12.0−15.1 GHz, for 10, 5, and 2 wt % loading, respectively. Similar phenomenon has been found for the composites of MWNT and other nanoscale material composites.[4,13] These results are of importance since the absorption peak frequency ranges of the SWNT composites can be tuned easily by changing the SWNT concentrations in the matrix, and thus a broad-band absorption design could be achieved using a multilayered absorbing structure.[19] The microwave absorption of these SWNT composites is considerably better than that of MWNTs/epoxy,[12,35] and comparable with that of MWNT/PET composites[13] where MWNTs were prepared by CVD method using Fe/Ai_2O_3 catalyst. Also, it is worth noting that the radar absorption is even better than that of iron fiber/epoxy composite with 20 vol % iron fiber.[36]

3.3. Radar Absorption Mechanism and Theoretical Simulation. Attenuation of microwave energy may occur due to either the dielectric loss or/and magnetic loss. According to transmission line theory,[37] when the electromagnetic wave transmits through a medium, the reflectivity is affected by many factors such as permittivity, permeability, sample thickness, and electromagnetic wave frequency. In order to better understand the microwave absorption results and investigate the intrinsic reasons for the absorption, we independently measured the relative complex permittivity and permeability of the SWNT/SCPU composites using the *T*/*R* coaxial line method as described in the Experimental Section. The permittivity results are shown in Figure 5. It is clearly seen that both the real and imaginary parts of the permittivity ϵ increase significantly with increasing SWNT loading, which is consistent with the results of other studies for SWNT[11,38] and MWNT[13,14,16,17,39−42] composites. But compared with the much increased complex permittivity, the complex permeability (not shown) of the composites is almost the same as that of pure SCPU sample, indicating no (minor) magnetic loss contribution from SWNT samples to the microwave absorption observed (also see below).

With these data, we then simulated the reflection loss using the transmission line theory. The reflection loss of EM radiation, R (dB), under normal wave incidence at the surface of a single-

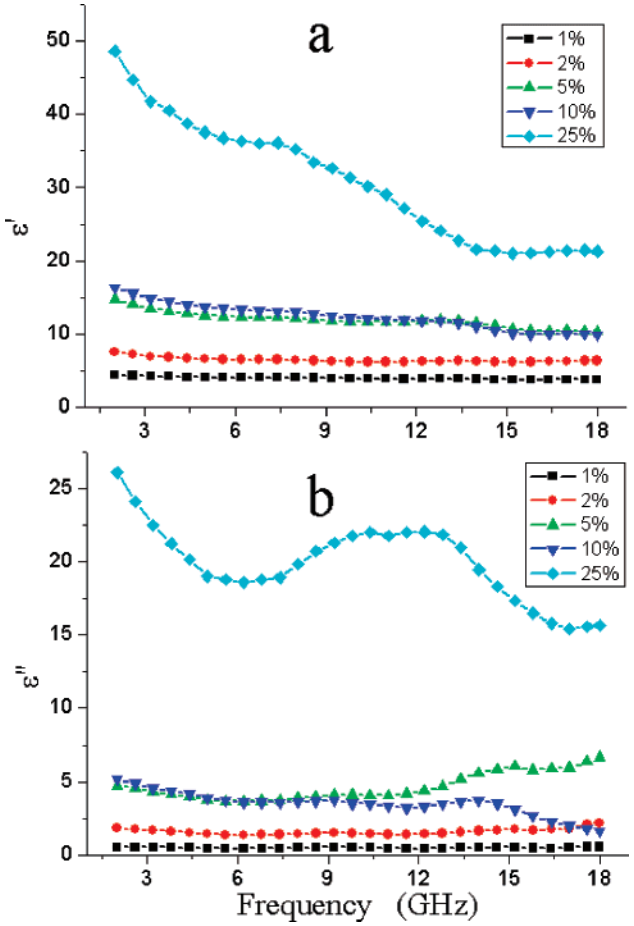

Figure 5. Real (ϵ') (a) and imaginary (ϵ'') (b) parts of the relative complex permittivity of SWNTs/SCPU composites with different loadings.

layer material backed by a perfect conductor can be defined as[37]

$$R = 20 \log\left|\frac{Z_{in} - Z_0}{Z_{in} + Z_0}\right| \quad (5)$$

where Z_0 is the characteristic impedance of free space,

$$Z_0 = \sqrt{\frac{\mu_0}{\epsilon_0}} \quad (6)$$

Z_{in} is the input impedance at the interface of free space and material,

$$Z_{in} = \sqrt{\frac{\mu_0 \mu}{\epsilon_0 \epsilon}} \tanh(j2\pi f \sqrt{\mu_0 \mu \epsilon_0 \epsilon} d) \quad (7)$$

where f is the frequency of the EM wave, d is the thickness of the material, ϵ is the relative permittivity, and μ is the relative permeability. The simulations of the reflection loss of the SWNTs/SCPU composites are shown in Figure 6.

In the view of the complexity of EM absorption, the theoretical results in Figure 6 agree reasonably well with the experimental results shown in Figure 4 in both the curve pattern and absolute values. For example, the simulation found the 5 wt % SWNT loading composite gave the highest microwave absorption for various loadings of SWNTs with 18.5 dB at 10.3 GHz, rather close to the experimental result (22 dB at 8.8 GHz), considering the complication of EMI.

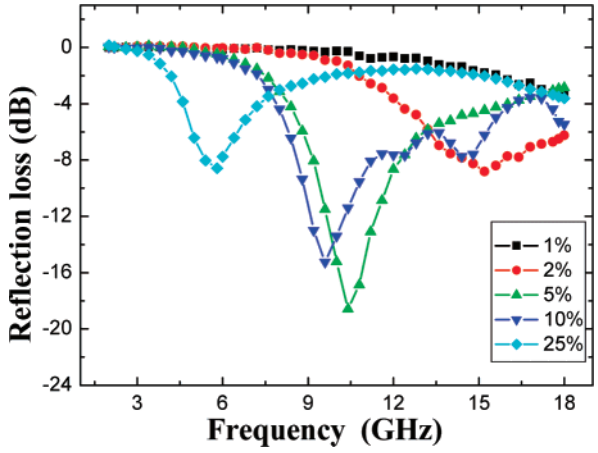

Figure 6. Simulation of reflection loss of SWNTs/SCPU composites using the transmission line theory.

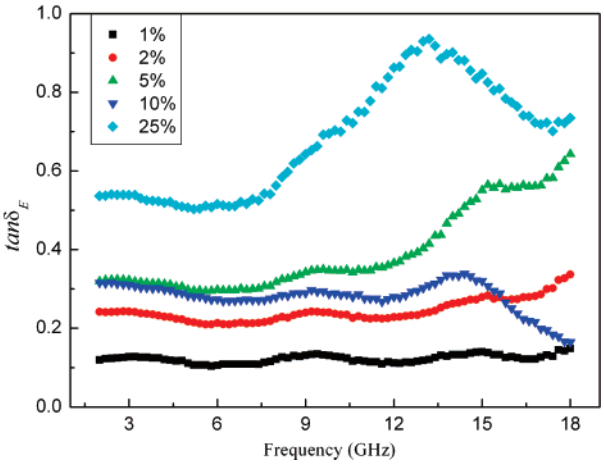

Figure 7. Dielectric loss (tan $\delta_E = \epsilon''/\epsilon'$) of the SWNT/PCPU samples in the microwave frequency range.

According to eqs 5 and 7, the condition minimizing reflection of incident plane wave (best absorption) happens when Z_{in} is most close to the constant Z_0, e.g., the permeability and permittivity of the composite match most as eq 7 indicates. As the complex permittivity of the composite increases significantly with increasing SWNT loading, we can see that for Z_{in} being closest to Z_0 (e.g., best absorption), the best reflection-loss frequency thus would decrease as eq 7 indicates. This also indicates that when the SWNT loading is 5%, Z_{in} should match Z_0 (where the permeability and permittivity of the composite match most as eq 7 indicates) most as compared to other SWNT loadings for our composites. Note the percolation point was 3.4 wt % from the conductivity study above, close to the loading of SWNTs with the best microwave absorption. It is well-known that percolation behavior corresponds to a phase transition from an insulator state to a conducting state for the composites around the percolation point. Although more data points need to be done to study the absorption for the composites with loading around 5 wt % for the best absorption, such as more data points from 3 to 8 wt %, we suspect that for these dielectric-loss microwave-absorbing materials the percolation point might have some direct relationship with the loading for the best absorption.

There are two possible contributions for microwave absorption, namely, dielectric loss and magnetic loss. We have also calculated both the dielectric tangent loss (tan $\delta_E = \epsilon''/\epsilon'$) and the magnetic tangent loss (tan $\delta_M = \mu''/\mu'$) based on the permeability and permittivity of the composite measured as

above. The value of the dielectric loss tangent increases with the increase of SWNT loading and is as high as 0.9 for the composite with 25 wt % loading (Figure 7). But the value of the magnetic tangent loss shows only very small fluctuation (in ± 0.2) around 0 (not shown). Furthermore, for all the composites with different SWNT loadings, the dielectric loss tangent tan δ_E is much larger than the magnetic loss tangent tan δ_M. Thus the main contribution for the microwave absorption should come from the dielectric loss.

In view of the design of a whole microwave bandwidth absorption, a multilayered sandwich structure[19] can be made by delicately altering the intrinsic properties of every layer. As an example, those with 2, 5, and 10 wt % loading each have already 2−3 GHz absorbing bandwidth for over 10 dB absorption. The total bandwidth of these three composites could cover almost the whole frequency range from ∼6−15 GHz. Considering the absorption peak could be easily tuned by changing the loading of SWNTs, with more optimization of the composites for absorption and multilayered sandwich structure design,[19] we believe that the SWNTs/SCPU composites shall have great potential for broad bandwidth radar wave absorbing materials.

4. Conclusions

Processable SWNTs/PU composites have been fabricated, and their microwave-absorbing properties have been studied in the range of 2−18 GHz. Among the composites with different SWNT loadings from 0 to 25 wt %, the composite having a 5 wt % loading shows the best absorption peak value (22 dB at 8.8 GHz). The main contribution for the microwave absorption comes from the dielectric loss rather than the magnetic loss. Theoretical calculation of microwave absorption using the transmission line theory from permittivity and permeability data agrees reasonably well with the experimental results. Considering the absorption peak could be easily tuned by changing the loading of SWNTs, these processable composite materials may have great potential for broad bandwidth radar wave absorbing applications.

Acknowledgment. The authors gratefully acknowledge the financial support from MoST (No. 2006CB0N0702), MoE (No. 20040055020), the NSF (No. 20644004) of China and the NSF (Nos. 07JCYBJC03000 and 06TXTJJC14603) of Tianjin City. Z. Liu and G. Bai contributed equally to this work.

References and Notes

(1) Chen, Y. J.; Cao, M. S.; Wang, T. H.; Wan, Q. *Appl. Phys. Lett.* **2004**, *84*, 3367−3369.
(2) Wadhawan, A.; Garrett, D.; Perez, J. M. *Appl. Phys. Lett.* **2003**, *83*, 2683−2685.
(3) Yang, Y. L.; Gupta, M. C.; Dudley, K. L.; Lawrence, R. W. *Adv. Mater.* **2005**, *17*, 1999−2003.
(4) Zhang, X. F.; Dong, X. L.; Huang, H.; Liu, Y. Y.; Wang, W. N.; Zhu, X. G.; Lv, B.; Lei, J. P.; Lee, C. G. *Appl. Phys. Lett.* **2006**, *89*, 053115-1-3.
(5) Baughman, R. H.; Zakhidov, A. A.; de Heer, W. A. *Science* **2002**, *297*, 787−792.
(6) Dresselhaus, M. S. *Nature* **2004**, *432*, 959−960.
(7) Wong, E. W.; Sheehan, P. E.; Lieber, C. M. *Science* **1997**, *277*, 1971−1974.
(8) Holt, J. K.; Park, H. G.; Wang, Y. M.; Stadermann, M.; Artyukhin, A. B.; Grigoropoulos, C. P.; Noy, A.; Bakajin, O. *Science* **2006**, *312*, 1034−1037.
(9) Minoux, E.; Groening, O.; Teo, K. B. K.; Dalal, S. H.; Gangloff, L.; Schnell, J. P.; Hudanski, L.; Bu, I. Y. Y.; Vincent, P.; Legagneux, P.; Amaratunga, G. A. J.; Milne, W. I. *Nano Lett.* **2005**, *5*, 2135−2138.
(10) Zhang, M.; Fang, S. L.; Zakhidov, A. A.; Lee, S. B.; Aliev, A. E.; Williams, C. D.; Atkinson, K. R.; Baughman, R. H. *Science* **2005**, *309*, 1215−1219.
(11) Li, N.; Huang, Y.; Du, F.; He, X.; Lin, X.; Gao, H.; Ma, Y.; Li, F.; Chen, Y.; Eklund, P. C. *Nano Lett.* **2006**, *6*, 1141−1145.
(12) Che, R. C.; Peng, L. M.; Duan, X. F.; Chen, Q.; Liang, X. L. *Adv. Mater.* **2004**, *16*, 401−405.
(13) Fan, Z. J.; Luo, G. H.; Zhang, Z. F.; Zhou, L.; Wei, F. *Mater. Sci. Eng., B* **2006**, *132*, 85−89.
(14) Kim, H. M.; Kim, K.; Lee, C. Y.; Joo, J.; Cho, S. J.; Yoon, H. S.; Pejakovic, D. A.; Yoo, J. W.; Epstein, A. J. *Appl. Phys. Lett.* **2004**, *84*, 589−591.
(15) Watts, P. C. P.; Hsu, W. K.; Barnes, A.; Chambers, B. *Adv. Mater.* **2003**, *15*, 600−603.
(16) Xiang, C. S.; Pan, Y. B.; Liu, X. J.; Sun, X. W.; Shi, X. M.; Guo, J. K. *Appl. Phys. Lett.* **2005**, *87*,123103-1-3.
(17) Yang, Y. L.; Gupta, M. C. *Nano Lett.* **2005**, *5*, 2131−2134.
(18) Ma, C. C. M.; Huang, Y. L.; Kuan, H. C.; Chiu, Y. S. *J. Polym. Sci., Part B: Polym. Phys.* **2005**, *43*, 345−358.
(19) Park, K. Y.; Lee, S. E.; Kim, C. G.; Han, J. H. *Compos. Sci. Technol.* **2006**, *66*, 576−584.
(20) Joo, J.; Epstein, A. J. *Appl. Phys. Lett.* **1994**, *65*, 2278−2280.
(21) Dalmas, F.; Chazeau, L.; Gauthier, C.; Masenelli-Varlot, K.; Dendievel, R.; Cavaille, J. Y.; Forro, L. *J. Polym. Sci., Part B: Polym. Phys.* **2005**, *43*, 1186−1197.
(22) Costa, L. C.; Henry, F.; Valente, M. A.; Mendiratta, S. K.; Sombra, A. S. *Eur. Polym. J.* **2002**, *38*, 1495−1499.
(23) Chung, D. D. L. *Carbon* **2001**, *39*, 279−285.
(24) Chiou, J. M.; Zheng, Q. J.; Chung, D. D. L. *Composites* **1989**, *20*, 379−381.
(25) Koerner, H.; Price, G.; Pearce, N. A.; Alexander, M.; Vaia, R. A. *Nat. Mater.* **2004**, *3*, 115−120.
(26) Liu, Z.; Bai, G.; Huang, Y.; Ma, Y.; Du, F.; Li, F.; Guo, T.; Chen, Y. *Carbon* **2007**, *45*, 821.
(27) Li, F. X.; Liu, Z. F.; Liu, X. P.; Yang, X. Y.; Chen, S. N.; An, Y. L.; Zuo, J.; He, B. L. *Macromolecules* **2005**, *38*, 69−76.
(28) Du, F.; Ma, Y.; Lv, X.; Huang, Y.; Li, F.; Chen, Y. *Carbon* **2006**, *44*, 1327−1330.
(29) Garboczi, E. J.; Snyder, K. A.; Douglas, J. F.; Thorpe, M. F. *Phys. Rev. E* **1995**, *52*, 819−828.
(30) Obukhov, S. P. *Phys. Rev. Lett.* **1995**, *74*, 4472−4475.
(31) Bryning, M. B.; Islam, M. F.; Kikkawa, J. M.; Yodh, A. G. *Adv. Mater.* **2005**, *17*, 1186−1191.
(32) Sandler, J.; Shaffera, M. S. P.; Prasseb, T.; Bauhoferb, W.; Schulte, K.; Windle, A. H.; *Polymer* **1999**, *40*, 5967−5971.
(33) Munson-McGee, S. H. *Phys. Rev. B* **1991**, *43*, 3331−3336.
(34) Grossiord, N.; Loos, J.; Regev, O.; Koning, C. E. *Chem. Mater.* **2006**, *18*, 1089−1099.
(35) Che, R. C.; Zhi, C. Y.; Liang, C. Y.; Zhou, X. G. *Appl. Phys. Lett.* **2006**, *88*, 033105.
(36) Wu, M. Z.; He, H. H.; Zhao, Z. S.; Yao, X. *J. Phys. D: Appl. Phys.* **2000**, *33*, 2398−2401.
(37) Michielssen, E.; Sajer, J.; Ranjithan, S.; Mittra, R. *IEEE Trans. Microwave Theory Tech.* **1993**, *41*, 1024−1030.
(38) Kim, B.; Lee, J.; Yu, I. *J. Appl. Phys.* **2003**, *94*, 6724−6728.
(39) Grimes, C. A.; Dickey, E. C.; Mungle, C.; Ong, K. G.; Qian, D. *J. Appl. Phys.* **2001**, *90*, 4134−4137.
(40) Wu, J. H.; Kong, L. B. *Appl. Phys. Lett.* **2004**, *84*, 4956−4958.
(41) Watts, P. C. P.; Ponnampalam, D. R.; Hsu, W. K.; Barnes, A.; Chambers, B. *Chem. Phys. Lett.* **2003**, *378*, 609−614.
(42) Wang, L.; Dang, Z. M. *Appl. Phys. Lett.* **2005**, *87*, 042903-1-3.